electronics

MDPI

Article

Robust Spectrum Sensing Detector Based on MIMO Cognitive Radios with Non-Perfect Channel Gain

Muthana Al-Amidie [1,2,*], Ahmed Al-Asadi [1,3], Amjad J. Humaidi [4], Ayad Al-Dujaili [5], Laith Alzubaidi [6,7,*], Laith Farhan [8], Mohammed A. Fadhel [9], Ronald G. McGarvey [10] and Naz E. Islam [1]

1 Faculty of Electrical Engineering and Computer Science, University of Missouri, Columbia, MO 65211, USA; aaabc2@mail.missouri.edu (A.A.-A.); islamn@missouri.edu (N.E.I.)
2 Faculty of Electrical Engineering, University of Babylon, Babylon 11707, Iraq
3 Faculty of Electrical Engineering, University of Technology, Baghdad 10001, Iraq
4 Control and Systems Engineering Department, University of Technology, Baghdad 10001, Iraq; Amjad.J.Humaidi@uotechnology.edu.iq
5 Faculty of Electrical Engineering Technical College, Middle Technical University, Baghdad 10001, Iraq; ayad.qasim@mtu.edu.iq
6 School of Computer Science, Queensland University of Technology, Brisbane, QLD 4000, Australia
7 Al-Nidhal Campus, University of Information Technology and Communications, Baghdad 00964, Iraq
8 School of Engineering, Manchester Metropolitan University, Manchester M1 5GD, UK; l.al-bayati@mmu.ac.uk
9 College of Computer Science and Information Technology, University of Sumer, Thi Qar 64005, Iraq; Mohammed.a.fadhel@uoitc.edu.iq
10 Faculty of Industrial Engineering Department and School of Public Affairs, University of Missouri, Columbia, MO 65211, USA; mcgarveyr@missouri.edu
* Correspondence: mkidn6@mail.missouri.edu (M.A.-A.); laith.alzubaidi@hdr.qut.edu.au (L.A.)

Abstract: The spectrum has increasingly become occupied by various wireless technologies. For this reason, the spectrum has become a scarce resource. In prior work, the authors have addressed the spectrum sensing problem by using multi-input and multi-output (MIMO) in cognitive radio systems. We considered the detection and estimation framework for MIMO cognitive network where the noise covariance matrix is unknown with perfect channel state information. In this study, we propose a generalized likelihood ratio test (GLRT) for the spectrum sensing problem in cognitive radio where the noise covariance matrix is unknown with non-perfect channel state information. Two scenarios are examined in this study: (i) in the first scenario, the sub-optimal solution of the worst case of the system's performance is considered; (ii) in the second scenario, we present a robust detector for the MIMO spectrum sensing problem. For both scenarios, the Bayesian approach with a generalized likelihood ratio test based on the binary hypothesis problem is used. From the results, it can be seen that our approach provides the best performance in the spectrum sensing problem under specified assumptions. The simulation results also demonstrate that our approach significantly outperforms other state-of-the-art spectrum sensing detectors when the channel uncertainty is addressed.

Keywords: cognitive radio; uncertainty channel state information; multi-input and multi-output; convex optimization; Bayesian technique; generalized likelihood ratio detector

Citation: Al-Amidie, M.; Al-Asadi, A.; Humaidi, A.J.; Al-Dujaili, A.; Alzubaidi, L.; Farhan, L.; Fadhel, M.A.; McGarvey, R.G.; Islam, N.E. Robust Spectrum Sensing Detector Based on MIMO Cognitive Radios with Non-Perfect Channel Gain. *Electronics* **2021**, *10*, 529. https://doi.org/10.3390/electronics10050529

Academic Editors: Adam Glowacz, Muhammad Irfan and Thompson Sarkodie-Gyan

Received: 14 January 2021
Accepted: 19 February 2021
Published: 24 February 2021

1. Introduction

High-speed data services with high quality of service (QoS) are responding to expanding demand by end-users, leading to many challenges in establishing reliable services in current 3G/4G wireless communication systems [1]. Since the spectrum has become a valuable resource for communication applications, it has also become essential to use the spectrum efficiently. However, McHenry et al. [1] report an extremely low efficiency for spectrum use on the geographic and temporal RF spectrum, and for that reason, the demand for good use of RF spectrum has increased and motivated researchers to find the best solutions for this problem. A promising approach to address the inefficient spectrum use is the cognitive radio (CR) [2–9], an attractive and novel communications technology that can

be used to enhance the scarce natural resources by efficiently using the spectrum. In a network, the spectrum is usually managed by the Federal Communication Commission (FCC) and can be shared between licensed primary users and unlicensed secondary users [10–14].

Spectrum sensing [15–19] is considered the key to CR in which the secondary user (SU) can identify whether or not the licensed primary user (PU) is using a wireless communication channel in CR networks. A reliable spectrum sensing step is an important stage in detecting a spectrum of holes that can be consequently saturated with the SU. In this case, many different techniques have been produced to sense the spectrum. Reusing the unoccupied licensed spectrum by unlicensed users in CR requires an efficient technique to detect the presence of free spectrum without causing interference between the users, as explained with more detail in [20,21]. Achieving reliable communication also requires an efficient technique for avoiding interference between the unlicensed user and the licensed user. This can be established by improving the parameters for the transmission or reception sides in the CR [8,22,23].

The spectrum sensing problem is an important challenge in CR. Thus, many researchers have recently studied this problem. Many techniques were proposed to solve this problem, the most widely used of which is the energy detector (ED), which represents a simple signal detector in spectrum sensing [24]. However, ED's performance is still inefficient when there is an error in noise or in channel state information (CSI) compared with other techniques. ED is also a method that depends on a hypothesis test (HT) [25,26].

In spectrum sensing, two or more phases have to be obtained to recognize the signal, so HT tests can be seen in this work [27] that the ED is an essential test in this problem. HT can also be invoked in many applications such as multiple model order selections [28–30], nonlinear regression [31], and many others. The use of a suitable statistic test is considered a significant step in HT, i.e., the main goal in achieving an efficient detector is to increase detection probability such as [32,33] in wireless communication.

Using multiple transmit and receive antennas can raise the channel capacity without needing to add additional power or bandwidth [34]. This was first studied in [35], which clarifies the capacity issue for a single-user with a Gaussian channel; and then in [36] multiple users have been proposed. MIMO has recently become the most important technique to achieve good accuracy between users in spectrum sensing wireless transmission and has been widely exploited in wireless communication [37,38].

Transmitting a signal over multi-antenna wireless links is affected by an additive interfering signal. Particularly when the interferer is found near the transmitter, interference will remain an unknown source for the receiver even though these effects are known by the transmitter. Moreover, if there is perfect CSI between the transmitter and receiver, then this technique is known as Dirty Paper Coding (DPC), in which the interference can be significantly decreased [39–42]. Several optimal detectors are proposed in [43] for non-antipodal signaling spectrum sensing-based MIMO CR with uncertainty in the channel. The channel coefficients are modeled ellipsoidal uncertainty sets while considering the nominal channel estimates as the ellipsoidal center. Thus, PU's spectrum detection problem is formulated as a second-order cone program (SOCP). A closed-form solution is used to solve this problem in this approach. This work also presents a multi-criterion robust detector (MRD) and a relaxed robust detector (RRD) for PU's spectrum sensing in CSI uncertainty scenarios. Based on those assumptions, the proposed approach's results show superior performance for the proposed cooperative detectors compared with the common detectors.

Moreover, an eigenvalue perturbation theory is used as in [44] to obtain the signal covariance matrix in this proposed approach. Subsequently, a novel scheme of spectrum detection is derived by exploiting an uncertainty signal covariance matrix for non-coherent spectrum sensing using CR networks. This problem is formulated using an optimization framework in which the generalized likelihood ratio test (GLRT) [45] based robust test used statistic detector (RTSD) and robust estimator-correlator detector (RECD) towards PU detection is involved. This closed-form expression is performed for the RTSD and RECD to

solve this problem, the optimization problem, with using the Karush-Kuhn-Tucker (KKT) conditions as problem constraints.

In [32], the binary hypothesis problem of spectrum sensing in multiple antenna CR is addressed using the prior information for unknown parameters. Bayesian technique with proper prior distribution is exploited to derive the corresponding detector for three varied scenarios with appropriate distribution for the unknown parameters. The channel uncertainty information is assumed to be available; besides this, unknown noise variance also exists. The iterative expectation-maximization method is used to estimate unknown parameters. Under certain assumptions, this work shows that using Bayesian techniques with GLRT approach gives acceptable results where an observed data samples is assumed as a finite number.

In this paper, we propose a mathematical model for the GLRT detector for spectrum sensing in CR. This model assumes imperfect CSI with unknown noise covariance. Two separate scenarios are addressed in this paper. The first scenario assumes non-perfect CSI is available while the noise covariance matrix is unknown to the SU. In this case, we derive the sub-optimal detector using a generalized likelihood ratio test with a Bayesian approach. This solution replaces the channel uncertainty with a specific matrix based on its location in the closed-form posterior probability expression for the observed covariance matrix. Next, the channel uncertainty in CSI and noise covariance are still unknown, which need to be estimated for the unauthorized user. In this scenario, we derive a robust detector that is a more reliable solution for spectrum sensing when channel uncertainty is nonperfect. This approach suggests a robust solution for the optimization problem to estimate the unknown parameters for both the noise covariance matrix and the channel uncertainty. Since the resulting optimization problem is challenging to solve, for reasons that will be explained later in subsequent sections, an iterative optimization technique is used to solve the problem and estimate the unknown parameters of the observed distribution. The original problem is divided into two sub-optimization problems in which a maximum a posteriori probability (MAP) method is used.

The main contributions of this paper are as follows:

(1) Observed data vectors in CR with multicell multiple groups at the secondary users are generated while maintaining the SNR levels with range values at the primary users. Then, the Bayesian method is used to assume priors for the unknown probabilistic parameters to extract a posterior probability distribution vector for the observation data samples of the CR system.
(2) We involve the MAP method to determine the posterior probability distribution expression for the unknown probabilistic parameter of the observation data to extract unknown matrices for the distribution parameters.
(3) We present two approaches to address the channel uncertainty and the noise covariance matrix that complicate the resultant optimization problem. The solution for this problem is examined under different approaches; this problem is solved by a sub-optimal solution in the first approach while a robust solution is used in the second approach.
(4) We prove that our approaches in the spectrum sensing problem based on the assumptions are effective methods to address this the uncertainty.

The outline of the rest of the paper is as follows: Section 2 shows a brief review of the B-GLRT approach for the independent and identically distributed (i.i.d.) random variables. Section 3 provides the system descriptions. Section 4 demonstrates the methodology under different assumptions. In Section 5, we show the proposed performance compared with state-of-the-art detectors based on computational testing. The last section provides concluding remarks.

Notation 1. *We use lightface letters for scalars, Boldface uppercase letters for matrices and boldface lowercase letters for vectors. The operation* $\|\cdot\|$ *denotes the norm,* $(\cdot)^H$ *is the conjugate transpose,* $\Gamma(\cdot)$ *refers to the gamma function,* $(\cdot)^*$ *denotes the conjugate,* $|\cdot|$ *is the determinant, diag* $(\cdot)$ *is the diagonal matrix,* $E[\cdot]$ *is the expected value, denotes the trace and* $etr(\cdot) = \exp trace(\cdot)$.

2. Spectrum Sensing Detector

The GLRT detector is considered to be an optimal solution in the hypothesis testing problem where the data signal has large samples. When the signal has a small sample size, the detection problem becomes a significant challenge to be solved. Based on [46], a Bayesian approach has been used to solve the detection problem where the signal sample is finite. The framework for the Bayesian approach and generalized likelihood ratio test (B-GLRT) is considered an optimal solution to the finite sample problem, which is also considered the combination for estimating the model parameters and detecting the signal. Moreover, $f(\mathbf{X}|\Theta_0)$ and $f(\mathbf{X}|\Theta_1)$ represent the density functions under H_0 and H_1 null and alternative hypothesis respectively [46,47]. Θ_0 and Θ_1 the unknown parameters. Assume further that the unknown parameters have prior distributions $f(\Theta_0)$ and $f(\Theta_1)$, respectively. The detection/estimation problem can be defined as mentioned in [46]:

$$\xi = \{\delta(H_1|\mathbf{x}), \delta(H_0|\mathbf{x}), f(\hat{\Theta}_1|\mathbf{x}, H_1), f(\hat{\Theta}_0|\mathbf{x}, H_0)\}, \tag{1}$$

Thus, the conditional risk of each hypothesis can also be defined as

$$\delta(\xi|H_i) = \int \left(f(H_0|\mathbf{x}) \int f(\hat{\Theta}_0|\mathbf{x}) \mathbb{A}_{0i}(\hat{\Theta}_0, \mathbf{x}) d\hat{\Theta}_0 \right) d\mathbf{x} + \int \left(f(H_0|\mathbf{x}) \int f(\hat{\Theta}_1|\mathbf{x}) \mathbb{A}_{1i}(\hat{\Theta}_1, \mathbf{x}) d\hat{\Theta}_1 \right) d\mathbf{x}. \tag{2}$$

where

$$\mathbb{A}_{ji}(\hat{\Theta}_j, \mathbf{x}) = \int C_{ji}(\hat{\Theta}_j, \Theta_i) f(\mathbf{x}|H_i, \Theta_i) f(\Theta_i) d\Theta_i. \tag{3}$$

At the end, the optimization problem becomes:

$$\inf_{\xi} \delta(\xi|H_1), \quad \text{subject to} \quad \delta(\xi|H_1) \leqslant \rho^{'}, \tag{4}$$

$C_{ji}(\hat{\Theta}_j, \Theta_i)$ is the cost function and considered to be '1' as defined in [47], the level $\rho^{'}$ is considered the maximum value of error type I under hypothesis H_0. Maximum Likelihood Estimation (MLE) is considered one of the most important methods to estimate the parameters in GLRT detector. Simultaneously, the MAP estimator can be used as an optimal solution under a finite sample size for the model parameters estimation when the B-GLRT is involved in solving the spectrum sensing problem. In particular, in [47], the GLRT is given by.

$$\mathbf{LR} = \frac{f(\mathbf{x}; H_1, \hat{\Theta}_1)}{f(\mathbf{x}; H_0, \hat{\Theta}_0)} \begin{cases} H_0 & < \\ H_1 & \geq \end{cases} \zeta \tag{5}$$

While the linear ratio for B-GLRT can be described as:

$$\mathbf{LR} = \frac{f(\mathbf{x}; H_1, \hat{\Theta}_1) f(\hat{\Theta}_1)}{f(\mathbf{x}; H_0, \hat{\Theta}_0) f(\hat{\Theta}_0)} \begin{cases} H_0 & < \\ H_1 & \geq \end{cases} \zeta \tag{6}$$

where $\hat{\Theta}_0$ and $\hat{\Theta}_1$ denote the estimation parameters under H_0 and H_1, respectively, ζ is the threshold of detector. These parameters are defined based on the prior distribution as:

$$\hat{\Theta}_t = \underset{\Theta_t}{\text{argmax}} f(\mathbf{x}; H_t, \Theta_t) f(\Theta_t). \tag{7}$$

where t refers to the hypothesis case. t can be "0" which refers to the null hypothesis or "1" referring to an alternative hypothesis, $\hat{\Theta}_t$ denotes the MAP approach to estimate the unknown parameters under H_0 and H_1. The following posterior distributions show the model's parameter estimators:

$$f(\hat{\Theta}_{MAP_t}|\mathbf{X}, H_t) \propto f_{H_t}(\mathbf{X}|\hat{\Theta}_{MAP_t}) f(\hat{\Theta}_{MAP_t}). \tag{8}$$

3. System Descriptions

In this section, an MIMO CR network with a single secondary user is associated with N_r receiving antennas and N_t is transmitting antennas, as shown in Figure 1. In this work, the noise and data samples are assumed to be independent of each other under the alternative hypothesis H_1, and also since any scaling of the PU signal can directly affected on the channel gain. These assumptions do not lead to a loss of generality. In many engineering applications, it can be seen that the detection problem is addressed when an additive Gaussian noise and the channel error are present, such as in [32,48]. H_1 and H_0 are considered the hypotheses of the presence and absence of the signal, respectively. Thus, the basic system model for the observed data at the secondary side can be described as:

$$\mathbf{X} = \begin{cases} \eta & H_0 \\ \mathbf{HS} + \eta & H_1 \end{cases} \tag{9}$$

where $\mathbf{H} \in \mathbb{C}^{N_r \times N_t}$ is the MIMO channel matrix between N_r transmitting antennas at the primary side and N_r receiving antennas on the secondary side, $\mathbf{S} \in \mathbb{C}^{N_t \times L}$ is PU signal samples at transmitter antennas, and $\eta \in \mathbb{C}^{N_r \times L}$ is the matrix of complex additive noise samples with covariance matrix $\mathbf{R}_\eta$. $\mathbf{X} \in \mathbb{C}^{N_r \times L}$ is the observation signal which is the Gaussian distribution with mean value and covariance matrix corresponding to each hypothesis, and L represents the number of data samples. Based on these assumptions, the mathematics and derivation of the problem will be simple. From the CR system model as described in Equation (9), the instant signal for each receiving antenna can be equivalently described as,

$$\mathbf{x}_i = \mathbf{Hs} + \eta_i. \tag{10}$$

where $\mathbf{x}_i \in \mathbb{C}^{N_r \times 1}$ is a complex data samples that contains the observed values at the instant i corresponding to sending signal that is corrupted by the noise vector $\eta_i \in \mathbb{C}^{N_r \times 1}$ which is additive white Gaussian . Moreover, $\mathbf{x}_i = [\mathrm{x}_i(1), \mathrm{x}_i(2), \ldots, \mathrm{x}_i(L)], \quad \forall i \in [1, \ldots, N_r]$. The channel matrix is defined as $\mathbf{H} = [\mathbf{h}_1, \mathbf{h}_2, \ldots, \mathbf{h}_{N_r}]$. Due to several practical limitations, the actual channel matrix cannot be accurately gathered at the transmitter. Thus, it is subject to some error such that,

$$\mathbf{H} = \hat{\mathbf{H}} + \mathbf{U}. \tag{11}$$

where $\hat{\mathbf{H}} = [\hat{\mathbf{h}}_1, \hat{\mathbf{h}}_2, \ldots, \hat{\mathbf{h}}_{N_r}]^T \in \mathbb{C}^{N_r \times N_t}$ is the nominal channel matrix that is available at the secondary user and $\hat{\mathbf{U}}_m = [\hat{\mathbf{u}}_1, \hat{\mathbf{u}}_2, \ldots, \hat{\mathbf{u}}_{N_r}]^T \in \mathbb{C}^{N_r \times N_t}$ is the related uncertainty matrix. The objective of the fusion center is to choose the correct model from the following two possible hypotheses:

$$\begin{aligned} \mathbf{x}_i/H_0 &\sim \mathcal{CN}(\mu_0, \mathbf{\Gamma}_0) \\ \mathbf{x}_i/H_1 &\sim \mathcal{CN}(\mu_1, \mathbf{\Gamma}_1) \end{aligned} \tag{12}$$

The mean and the covariance matrix of the observation for each receiving antenna at the alternative hypothesis can be derived as follows:

$$\begin{aligned} \mu_1(k) &= E[\mathbf{x}_i/H_1] = E[\mathbf{Hs} + \eta_i] \\ &= E[\mathbf{Hs}] + E[\eta_i] = \mathbf{H}E[\mathbf{s}] = 0 \\ \Gamma_1(k) &= E[\mathbf{x}_i\mathbf{x}_i^H] = E[(\mathbf{Hs} + \eta_i)(\mathbf{Hs} + \eta)^H] \\ &= E[\mathbf{Hss}^H\mathbf{H}^H] + E[\eta_i\eta_i^H] + E[\mathbf{Hs}\eta_i^H] + E[\eta_i\mathbf{H}^H\mathbf{s}^H] \\ &= \mathbf{HH}^H + \Gamma_0. \end{aligned}$$

where $\mathbf{\Gamma}_1$ is equal to $\mathbf{HH}^H + \mathbf{R}\eta \in \mathbb{C}^{N_r \times N_r}$ and $\mathbf{\Gamma}_0$ is equal to $\mathbf{R}_\eta \in \mathbb{C}^{N_r \times N_r}$. The likelihood of the observation x_i corresponding to the alternative hypothesis $\mathcal{H}_0$ is given by:

$$\mathbf{p}(\mathbf{x}_i, \mathcal{H}_0) = \frac{exp(-\mathbf{x}_i \mathbf{\Gamma}_0 \mathbf{x}_i^H)}{\pi^{L+N_r N_t} |\mathbf{\Gamma}_0|} \tag{13}$$

while the likelihood of the observation x_i corresponding to the alternative hypothesis $\mathcal{H}_1$ is given by:

$$\mathbf{p}(\mathbf{x}_i, \mathcal{H}_1) = \frac{exp(-\mathbf{x}_i \mathbf{\Gamma}_1 \mathbf{x}_i^H)}{\pi^{L+N_r N_t} |\mathbf{\Gamma}_1|} \tag{14}$$

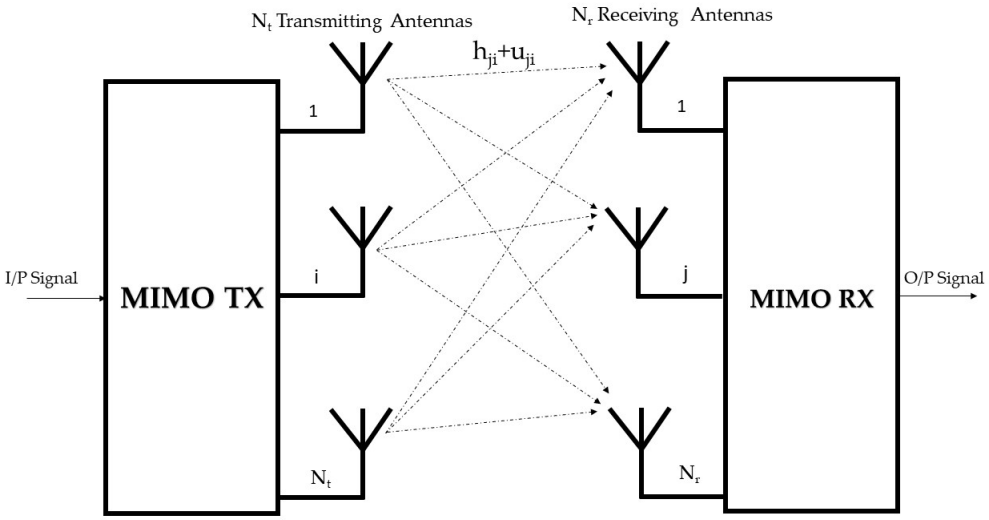

Figure 1. MIMO cognitive radio system model consisting of single PU with N_t transmitting antennas and single secondary user with N_r receiving antennas.

The article's flowchart is shown in Figure 2, where we first detect the MIMO cognitive signal to find the hypothesizes of the received signal. In the sequel, we exploit the above observation values to estimate the model parameters, in which simulated threshold can be determined and closely followed by the unknown parameters estimation part. Then, we apply the B-GLRT method to observation data samples with the estimated parameters to obtain the signal's hypothesis.

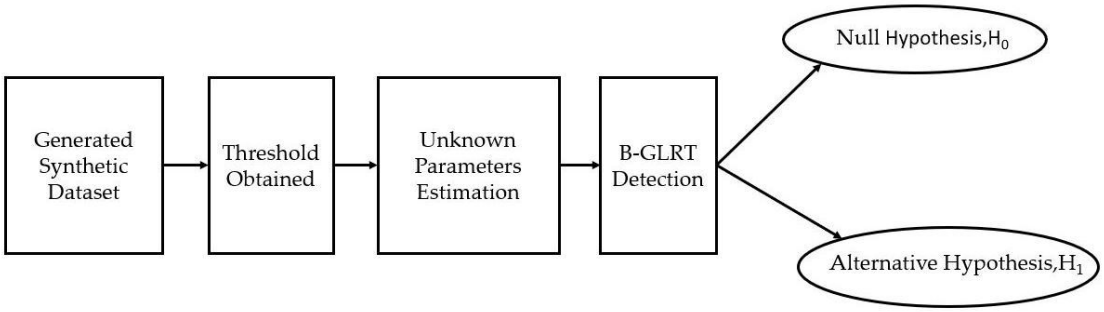

Figure 2. Algorithm flowchart.

4. Methodology

4.1. B-GLRT Detector for Unknown Noise Covariance Matrix with Perfect CSI (B-GLRT1)

In this part, we assume the channel uncertainty is known while the noise covariance matrix is unknown at the SU. Prior information for the noise distribution is assumed to be unknown at the SU. Now, we assume that the noise variance has an Inverse-Gamma prior

distribution with different values of shape ρ and scale parameter κ . Therefore, the expression of the prior distribution of the noise variance as shown in [32,33,49] is $\gamma^2 \sim$ Inv-Gamma (ρ, κ). In other words, a diagonal matrix $\mathbf{\Gamma}_0 = diag\ (\gamma^2_{0,1}, \ldots, \gamma^2_{0,N_r})$ present the noise covariance matrix, and each $\gamma^2_{0,i}$ is clearly modeled *a priori* probability using an Inverse-Gamma distribution with the shape parameter ρ_i and the scale parameter κ_i. Now, the Bayesian approach can be used in this case to determine the unknown model parameters when the finite observation sample is available. Here the channel matrix is supposed to be known while the noise variance is unknown for the SU. To obtain more elastic calculation, we applied the joint prior for the noise variance parameters as given by,

$$\begin{aligned} f\left(\gamma^2_{0,i}\right) &= f(\mathbf{\Gamma}_0) \\ &= \prod_{i=1}^{N_r} \frac{\kappa_i^{\rho_i}}{\Gamma(\rho_i)} \left(\gamma^2_{0,i}\right)^{-\rho_i - 1} \exp\left(\frac{-\kappa_i}{\gamma^2_{0,i}}\right). \end{aligned} \tag{15}$$

where $i = [1, \ldots, N_r]$, In order to obtain the values of unknown parameters in the null hypothesis, and since these parameters have prior knowledge based on the Bayesian theorem, the maximum *a posterior* probability can be involved in this case. This can be achieved by taking the log of Equation (8) followed by taking the maximum that is obtained by deriving the expression for the unknown variables, as shown in Equation (16) to achieve the MAP estimator. We explore the MAP method of the noise variance parameters under H_0 as follows:

$$\hat{\Theta}_0 | \mathbf{x}, H_0 = \text{Max}\{\log(f_{H_0}(\mathbf{x}|\Theta_0) f(\Theta_0))\} \tag{16}$$

Then the posterior distribution of noise variance can be shown as:

$$\hat{\mathbf{\Gamma}}_0 = \underset{\mathbf{\Gamma}_0}{\text{argmax}} [\log(f(\mathbf{X}; H_0, \mathbf{\Gamma}_0)) + \log(f(\mathbf{\Gamma}_0))]. \tag{17}$$

In the null hypothesis, $\mathbf{\Gamma}_0 = \mathbf{R}_\eta$. Thus, Equation (17) become Equation (18),

$$\hat{\mathbf{R}}_\eta = \underset{\mathbf{R}_\eta}{\text{argmax}} \left[\log(f(\mathbf{X}; H_0, \mathbf{R}_\eta)) + \log(f(\mathbf{R}_\eta))\right]. \tag{18}$$

It can be seen from the system model that the observation data at each secondary antenna follows a complex normal distribution with density:

$$\begin{aligned} f_{H_0}(\mathbf{X}|\mathbf{\Gamma}_0) &= \prod_{j=1}^{L} f_{H_0}(\mathbf{x}_j|\mathbf{R}_\eta) \\ &= \pi^{-N_r L} \left(\prod_{i=1}^{N_r} \gamma^2_{0,i}\right)^{-L} \exp\left\{-\sum_{i=1}^{N_r} \sum_{j=1}^{L} \frac{x^*_{ij} x_{ij}}{\gamma^2_{0,i}}\right\} \\ &= \pi^{-N_r L} \prod_{i=1}^{N_r} \left[(\gamma^2_{0,i})^{-L} \exp\left\{\frac{-1}{\gamma^2_{0,i}} \sum_{j=1}^{L} x^*_{ij} x_{ij}\right\}\right]. \end{aligned} \tag{19}$$

According to Equation (17), the log function can be taken after the multiplication between Equation (19) and Equation (15) and one can then take the derivative with respect to $\gamma^2_{0,i} > 0$, $i = [1, \ldots, N_r]$, to estimate the model parameter. It can be easily seen as follows:

$$\gamma^2_{0,i} = \frac{1}{L + \rho_i + 1} \left(\sum_{j=1}^{L} x^*_{ij} x_{ij} + \kappa_i\right). \tag{20}$$

for $i = [1, \ldots, N_r]$, (see Appendix 1 in our previous work [33] for more detail about the proof).

Under the alternative hypothesis, we obtain the MAP estimation of the noise covariance matrix in the hypothesis detection problem where the channel gain and its error are known. Based on Equation (16) the MAP estimation equation will be:

$$\hat{\Theta}_1 = \underset{\Theta_1}{\operatorname{argmax}} f(\mathbf{x}; H_1, \Theta_1) f(\Theta_1). \tag{21}$$

In the alternative hypothesis, $\mathbf{\Gamma}_1 = \mathbf{H}\mathbf{H}^H + \mathbf{\Gamma}_0$ represents the covariance matrix of the observation where the channel has known uncertainty as shown in Equation (11). $\mathbf{\Gamma}_0$ is also modeled as *a priori* using Equation (15). The density of $\mathbf{x}$ in the alternative hypothesis is given by:

$$f_{H_1}(\mathbf{x}; \mathbf{\Gamma}_0) = \pi^{-N_r} |\mathbf{\Gamma_1}|^{-1} \exp\left\{-\mathbf{x}^H \mathbf{\Gamma}_1^{-1} \mathbf{x}\right\}$$

where $\Gamma_1 = (\mathbf{H}\mathbf{H}^H + \mathbf{\Gamma}_0)^{-1}$. Thus, the data distribution under H_1 has density:

$$\begin{aligned} f_{H_1}(\mathbf{X}|\mathbf{R}_\eta) &= \pi^{-N_r} \left|\mathbf{H}\mathbf{H}^H + \mathbf{R}_\eta\right|^{-L} \\ &\quad \times \exp\left\{-\sum_{j=1}^{L} \mathbf{x}_j^H (\mathbf{H}\mathbf{H}^H + \mathbf{R}_\eta)^{-1} \mathbf{x}_j\right\} \\ &= \pi^{-N_r} \left|\mathbf{H}\mathbf{H}^H + \mathbf{R}_\eta\right|^{-L} etr\left\{-\mathbf{R}(\mathbf{H}\mathbf{H}^{\mathbf{H}} + \mathbf{R}_{\mathbf{J}})^{-\mathbf{1}}\right\}. \end{aligned} \tag{22}$$

Let $\mathbf{R}_h = \mathbf{H}\mathbf{H}^H$ be the channel covariance matrix which is known for the SU. We also define $\mathbf{R} = \sum_{j=1}^{L} \mathbf{x}_j \mathbf{x}_j^H$. Thus, the MAP method of the noise variance under H_1 is provided by determining the next optimization problem:

$$P1 : \underset{\mathbf{\Gamma}_1}{\operatorname{argmax}} \left[\log(f_{H_1}(\mathbf{X}|\mathbf{\Gamma}_1)) + \log(f(\mathbf{\Gamma}_0))\right]. \tag{23}$$

By substituting Equations (15) and (22) into Equation (23), P1 becomes:

$$\begin{aligned} P2 : \quad & \underset{\mathbf{\Gamma}_0}{\operatorname{argmax}} \left[\log f_{H_1}(\mathbf{X}|\mathbf{\Gamma}_1) + \log f(\mathbf{\Gamma}_0)\right] \\ &= \underset{\Gamma_0 : Diagonal}{\operatorname{argmax}} \left(L \log\left|\mathbf{\Gamma}_1^{-1}\right| - tr[\mathbf{R}\mathbf{\Gamma}_1^{-1}]\right. \\ &\quad \left. + (\rho + 1) \log\left|\mathbf{\Gamma}_0^{-1}\right| - tr[\mathbf{K}\Gamma_0^{-1}]\right). \end{aligned} \tag{24}$$

where $(\rho_1 = \cdots = \rho_{N_r} = \rho)$ are the hyperparameters of the conjugate priors and $\mathbf{K} = diag(\kappa_1, \ldots, \kappa_{N_r})$ is the diagonal matrix which represents the conjugate priors' hyperparameters. Since problem P2 is not convex it can be solved by successive convex approximation using an interior point method. Here we manipulate the formulation to obtain an equivalent convex optimization problem which can be easily solved by using a numerical semidefinite programming (SDP) optimization package such as in [50]. According to [51], the optimization problem is solved with a complexity of $\mathcal{O}((N_t + 1)^{1/2}(N_t + N_r + 1)(N_t + 1)^2)$ [52] in terms of system parameters. For more detail regarding the derivation, see Appendix A.1.

4.2. B-GLRT Detector for Unknown Noise Covariance Matrix with Non-Perfect CSI

We assume that the estimated channel is non-perfect with an unknown uncertainty matrix, and the noise covariance matrix is also assumed to be an unknown matrix for the SU. We use the same prior distribution for the noise variance as in Equation (15). According to the system model as given in Equation (10), the estimated value of noise covariance matrix in the null hypothesis still can be obtained by using Equation (20) while in the

alternative hypothesis, both channel uncertainty and noise covariance matrix must be estimated. Hence, the problem can be formulated as

$$\begin{aligned} P3: \quad & \underset{\substack{\mathbf{\Gamma}_0:Diagonal \\ \mathbf{\Gamma}_1 \geq 0}}{\operatorname{argmax}} \left[\log f_{H_1}(\mathbf{X}|\mathbf{\Gamma}_1) + \log f(\mathbf{\Gamma}_0)\right] \\ & = \underset{\Gamma_0:Diagonal}{\operatorname{argmax}} \left(L \log\left|\mathbf{\Gamma}_1^{-1}\right| - tr[\mathbf{R}\mathbf{\Gamma}_1^{-1}]\right. \\ & \left. + (\rho+1)\log\left|\mathbf{\Gamma}_0^{-1}\right| - tr[\mathbf{K}\Gamma_0^{-1}]\right). \end{aligned} \tag{25}$$

Then the objective is to maximize the likelihood-ratio (LR) subject to certain constraints, so $P3$ becomes.

$$\begin{aligned} P4 \quad : \quad & \underset{\Gamma_0:Diagonal}{\operatorname{argmax}} \left(L \log\left|(\widehat{\mathbf{R}}_h + \mathbf{\Delta R}_h) + \mathbf{\Gamma}_0\right|^{-1}\right. \\ & -tr[\mathbf{R}\Big((\widehat{\mathbf{R}}_h + \mathbf{\Delta R}_h) + \mathbf{\Gamma}_0\Big)_1^{-1}] \\ & \left. +(\rho+1)\log\left|\mathbf{\Gamma}_0^{-1}\right| - tr[\mathbf{K}\mathbf{\Gamma}_0^{-1}]\right). \end{aligned} \tag{26}$$

Here, we must maximize $f_{H_1}(\mathbf{x}|\mathbf{\Gamma}_0)$ because $f_{H_1}(\mathbf{x}|\mathbf{\Gamma}_0)$ is a function of $\Delta\mathbf{R}_h$ which is the channel error and has an effect on the maximization of LR. To find the value of $\Delta\mathbf{R}_h$ that maximizes $f_{H_1}(\mathbf{x}|\mathbf{\Gamma}_0)$, we can use the following approaches.

4.2.1. Sub-Optimal Solution, B-GLT2

In this solution, we substitute the value of $\mathbf{\Delta R}_h$ that gives the minimum value for $f_{H_1}(\mathbf{x}|\mathbf{\Gamma}_0)$ as shown in Equation (26), where $\mathbf{\Delta R}_h$ equal to $-\epsilon\mathbf{I}_M$ or $+\epsilon\mathbf{I}_M$ depending on the position of $\mathbf{\Delta R}_h$ in $f_{H_1}(\mathbf{x}|\mathbf{\Gamma}_0)$ or in case the values of $\mathbf{\Delta R}_h$ in$f_{H_1}(\mathbf{x}|\mathbf{\Gamma}_0)$ that lead to the minimum value of $f_{H_1}(\mathbf{x}|\mathbf{\Gamma}_0)$ are both $+\epsilon\mathbf{I}_M$. Thus,

$$\begin{aligned} f_{H_1}(\mathbf{x}|\mathbf{\Gamma}_0) = \pi^{-N_r}\left|(\widehat{\mathbf{R}}_h + \epsilon\mathbf{I}_M) + \mathbf{\Gamma}_0\right|^{-L} \\ etr\Big\{-\mathbf{R}(\widehat{\mathbf{R}}_\mathbf{h} + \epsilon\mathbf{I}_\mathbf{M}) + \mathbf{\Gamma_0})^{-\mathbf{1}}\Big\}, \end{aligned} \tag{27}$$

Therefore, the optimization problem can be seen in $P5$:

$$\begin{aligned} P5 \quad : \quad & \underset{\Gamma_0:Diagonal}{\operatorname{argmax}} \left(L \log\left|(\widehat{\mathbf{R}}_h + \epsilon\mathbf{I}_M) + \mathbf{\Gamma}_0\right|^{-1}\right. \\ & -tr[\mathbf{R}\Big((\widehat{\mathbf{R}}_h + \epsilon\mathbf{I}_M) + \mathbf{\Gamma}_0\Big)_1^{-1}] \\ & \left. +(\rho+1)\log\left|\mathbf{\Gamma}_0^{-1}\right| - tr[\mathbf{K}\mathbf{\Gamma}_0^{-1}]\right). \end{aligned} \tag{28}$$

The positive exponent means that the bounded matrix must be positive semidefinite (PSD). Due to the Hermitian operation of $\widehat{\mathbf{R}}_h$, this can be accomplished by setting the negative Eigenvalues of the resultant $\widehat{\mathbf{R}}_h + \epsilon\mathbf{I}_M$ to zero. Now, the problem can be solved based on Appendix A.2.

4.2.2. Robust Solution, B-GLT3

Returning to Equation (26), we can see that this problem consists of two optimization variables ($\Delta\mathbf{R}_h$, $\mathbf{\Gamma}_0$) . This can be difficult to solve as a single optimization problem. Thus, it can be solved using iterative optimization techniques following a similar procedure as in our previous work [53] and as following in [54]. The optimization problem becomes:

- Solving for $\mathbf{\Gamma}_0$: in this case, we assume that $\mathbf{\Gamma}_0$ is unknown and $\Delta\mathbf{R}_h$ is known and then solve for $\mathbf{\Gamma}_0$ as shown in *P6*.

$$\begin{aligned} P6 \quad : \quad & \underset{\Gamma_0}{\operatorname{argmax}}(L\log|\underbrace{(\widehat{\mathbf{R}}_h+\mathbf{\Delta R}_h)}_{\mathbf{R}_h}+\mathbf{\Gamma}_0|^{-1} \\ & -tr[\mathbf{R}(\underbrace{(\widehat{\mathbf{R}}_h+\mathbf{\Delta R}_h)}_{\mathbf{R}_h}+\mathbf{\Gamma}_0)^{-1}] \\ & +(\rho+1)\log\left|\mathbf{\Gamma}_0^{-1}\right|-tr[\mathbf{K}\mathbf{\Gamma}_0^{-1}]). \end{aligned} \tag{29}$$

  subject to

$$\mathbf{\Gamma_0} \geq 0,$$

  For additional details see Appendix A.2.

- Solving for $\Delta\mathbf{R}_h$: now we can assume that $\mathbf{\Gamma}_0$ is known and solve for $\Delta\mathbf{R}_h$. We also define that $\Re = \widehat{\mathbf{R}}_h + \mathbf{\Gamma}_0$, then the problem becomes:

$$\begin{aligned} P7 \quad : \quad & \underset{\Delta\mathbf{R}_h}{\operatorname{argmax}}(L\log|(\Re+\mathbf{\Delta R}_h)|^{-1} \\ & -tr[\mathbf{R}(\Re+\mathbf{\Delta R}_h)^{-1}] \\ & +(\rho+1)\log\left|\mathbf{\Gamma}_0^{-1}\right|-tr[\mathbf{K}\mathbf{\Gamma}_0^{-1}]). \end{aligned} \tag{30}$$

  subject to

$$\|\mathbf{\Delta R}_h\|_F \leq \epsilon,$$

  Appendix A.2 provides more detail on this derivation.

After estimating the model parameters Γ_0 and Γ_1 in both hypothesis, the detector expression is easily derived; this step starts with taking the log of Equation (6) as follows:

$$\begin{aligned} \text{LLR} = & \log(f_{H_1}(\mathbf{x}|\mathbf{\Gamma}_1)f(\mathbf{\Gamma}_1)) \\ & -\log(f_{H_0}(\mathbf{x}|\mathbf{\Gamma}_0)f(\mathbf{\Gamma}_0)). \end{aligned} \tag{31}$$

Then, the log of the posterior distribution can be:

$$\begin{aligned} \log(.)|H_0 = & -(L+\rho+1)\log(|\hat{\mathbf{\Gamma}}_0|) \\ & +tr(-\mathbf{R}\hat{\mathbf{\Gamma}}_0^{-1})-tr(\mathbf{K}\hat{\mathbf{\Gamma}}_0^{-1}). \end{aligned} \tag{32}$$

and

$$\begin{aligned} \log(.)|H_1 = & -(L+\rho+1)\log(|\hat{\mathbf{\Gamma}}_\mathbf{1}|) \\ & +tr(-\mathbf{R}\hat{\mathbf{\Gamma}}_1^{-1})-tr(\mathbf{K}\hat{\mathbf{\Gamma}}_1^{-1}). \end{aligned} \tag{33}$$

By substituting Equations (32) and (33) in Equation (31). Therefore, the detector is given by:

$$\mathrm{T}_1(\mathrm{B}-\mathrm{GLRT}) = (L+\rho+1)\log(\frac{|\hat{\mathbf{\Gamma}}_1|}{|\hat{\mathbf{\Gamma}}_0|})+tr(-\mathbf{R}\hat{\mathbf{\Gamma}}_1^{-1})-tr(-\mathbf{R}\hat{\mathbf{\Gamma}}_0^{-1})-tr(\mathbf{K}\hat{\mathbf{\Gamma}}_1^{-1})+tr(\mathbf{K}\hat{\mathbf{\Gamma}}_0^{-1}) \underset{H_0}{\overset{H_1}{\gtrless}} \zeta \tag{34}$$

In the next section, we test the performance of the proposed approach for two different simulation scenarios. In the first scenario, we have incorporated perfect channel information with an unknown noise covariance matrix, while in the second scenario, we have incorporated unknown noise covariance with imperfect CSI.

5. Numerical Evaluation

In this section, we explain our approach using synthetic data to clarify the performance of our design of the GLRT spectrum sensing algorithm where the channel uncertainty exists. In our simulation, the average received SNR at SU is modeled as shown in [33],

$$SNR = \log(tr(\mathbf{H}\mathbf{H}^H)) - \log(tr(\mathbf{\Gamma}_0)). \tag{35}$$

First, we show the impact of the channel uncertainty **U** in spectrum sensing where the noise parameters are also unknown and uncorrelated. As mentioned previously, the channel uncertainty is assumed to have deterministic values, while prior knowledge is assumed for the noise parameters. For these assumptions, we show the GLRT algorithm's performance based on the Bayesian approach that is defined by B-GLR1, and we show its performance compared with other proposed methods. These approaches are also compared with other state-of-the-art spectrum sensing detectors under the same assumptions, such as the ED.

As mentioned, the MIMO technique is considered in this paper with the number of receiving antennas N_r equal to 3 to receive several samples L equal to 20, the number of transmitting antennas N_t= 2. We also set the hyperparameter values of prior distributions parameter as the shape ($\rho_1 = \ldots = \rho_{N_r}$) equal to 2, and the scale **K** has different arbitrary values as diag [2, 1.5, 3]. The number of realizations is 5×10^4 in which the probability of false alarm (pfa) can be generated, and then the threshold value can be numerically obtained. In terms of SNR, Figure 3 illustrates the probability of missed detection (Pm) for the proposed approach. This figure also shows the comparison with common different detectors such as the maximum to minimum eigenvalue test (MME), energy with minimum eigenvalue test (EME) [55,56] as shown in Equations (36) and (37) respectively.

$$\mathrm{T}_{\zeta}(MME) = \frac{\lambda_{max}(\hat{\Gamma})}{\lambda_{min}(\hat{\Gamma})} \underset{H_0}{\overset{H_1}{\gtrless}} \zeta \tag{36}$$

$$\mathrm{T}_{\zeta(EME)} = \frac{\lambda_{av}(\hat{\Gamma})}{\lambda_{min}(\hat{\Gamma})} \underset{H_0}{\overset{H_1}{\gtrless}} \zeta \tag{37}$$

where λ_{max}, λ_{min}, and λ_{av} respectively denote the maximum, minimum, average eigenvalues of the covariance matrix ($\hat{\Gamma}$).

In this figure, the detector's performance can be shown within the SNR range between [–20 to 10] while a probability density function (pdf) = 5×10^{-1} and the finite sample number L equal to 20. The observation data is generated according to Equation (12) after estimating the noise covariance noise matrix for (B-GLRT1) or both the noise covariance matrix and the channel uncertainty (for the other proposed detectors). Using the sub-optimal solution and robust solution, the channel uncertainty can be obtained. In addition, for channel estimation, the noise covariance matrix is calculated using the same methods as for estimating the channel uncertainty. Following the estimation parameters, the detector can be used as shown in Equation (34) to assign the signal to one hypothesis. Clearly, four state-of-the-art detectors with three proposed detectors can be clarified in terms of SNR. It can also be seen that B-GLRT 1 outperforms other proposed detectors since it lies on the efficient frontier compared with other methods. Respective operating characteristic curves (ROC) can be seen in Figure 4. In this figure, we show the probability of detection (PD) versus the probability of false alarm using a range of values of pfa, SNR value is -3 dB, and the number of samples L equal to 10. In this figure, we assume that there is a range of false alarm probability values. For each value of this probability, the threshold is simulated, allowing us to obtain the threshold vectors as a function of the alarm probability values. We again observe that the proposed approach achieves efficient performance compared with other state-of-the-art detectors such as the Hadamard ratio test and the Sphericity test [57] shown in Equations (38) and (39) respectively. In addition, the results show that the optimal detector largely outperforms Hadamard ratio test

and Sphericity test, and we show that the proposed B-GLRT1 detector has an excellent performance compared with other proposed detectors:

$$\mathrm{T}_{\zeta}(HR) = \left(\prod_{j=1}^{N_r} \gamma_{jj}\right) |\Gamma|^{-1} \underset{H_0}{\overset{H_1}{\gtrless}} \zeta \tag{38}$$

$$\mathrm{T}_{\zeta}(ST) = \left(\frac{\sum_{j=1}^{N_r} \gamma_{jj}}{N_r}\right) |\Gamma|^{-(1/N_r)} \underset{H_0}{\overset{H_1}{\gtrless}} \zeta \tag{39}$$

where Γ is the covariance matrix. We also show the performance of proposed detectors in terms of the signal size. In Figure 5, the probability of missed detection (Pm) for each detector can be observed versus the number of samples L. In Figure 5, it can be shown that the proposed detectors have a significantly superior achievement relative to the other detectors where pfa is equal 5×10^{-1}, $N_r = 3$, $N_t = 2$ and the average SNR of –3 dB. It can be observed that the proposed detector performance has a significant improvement when the input samples increase. In addition, the proposed B-GLRT1 detector performs better than other detectors due to perfect CSI.

We next present another simulation to show the detectors' performance for more reliability when the signal sample size is large. In this section, Figure 6 clarifies the relation between the probability of detection against the probability of false alarm (pfa). From this figure, it can generally be observed that even though most detectors' performance has a significant improvement, the proposed detectors still maintain performance advantage compared with other detectors. It also shows that proposed detectors 'B-GLRT2', and 'B-GLRT3' have sufficient ability to be robust detectors against channel uncertainty. Moreover, to study the impact of the observed data samples size on the detectors' performance in this approach, the performance is determined as shown in Figure 7; this figure shows that spectrum sensing's achievement is raised when the observed data samples is high.

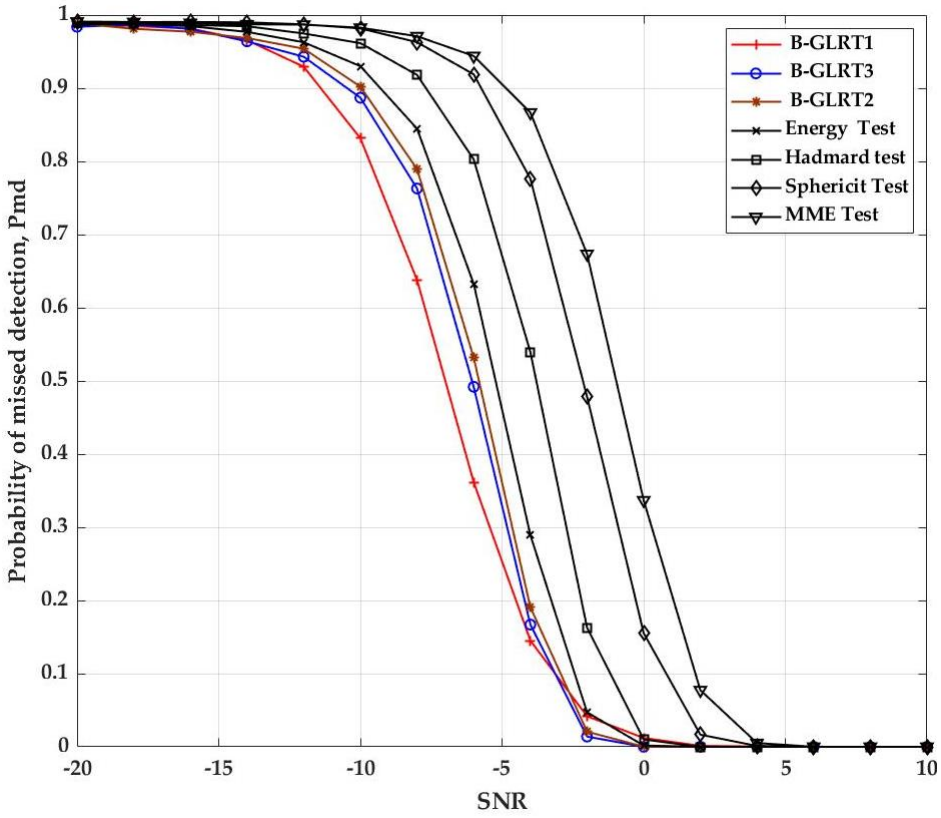

Figure 3. Probability of missed detection versus the SNR for $Pfa = 5 \times 10^{-1}$, $N_r = 3$ and $L = 20$.

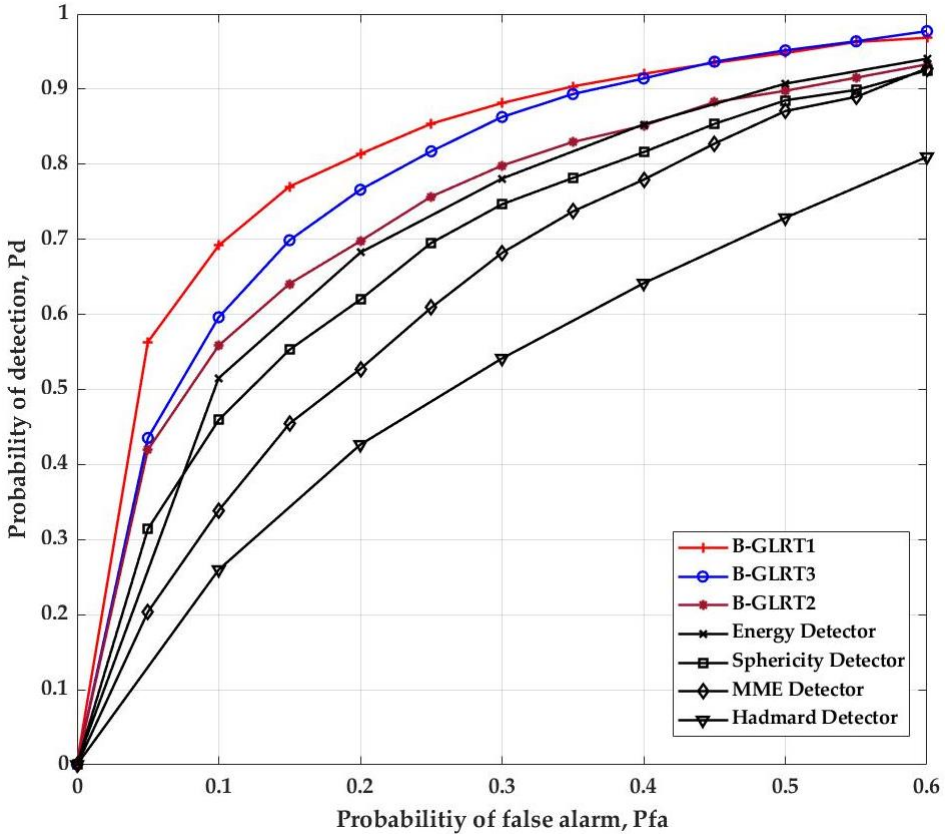

Figure 4. The ROC performance of the proposed B-GLRT where a SNR = –3 dB, N_r = 3 and L = 10.

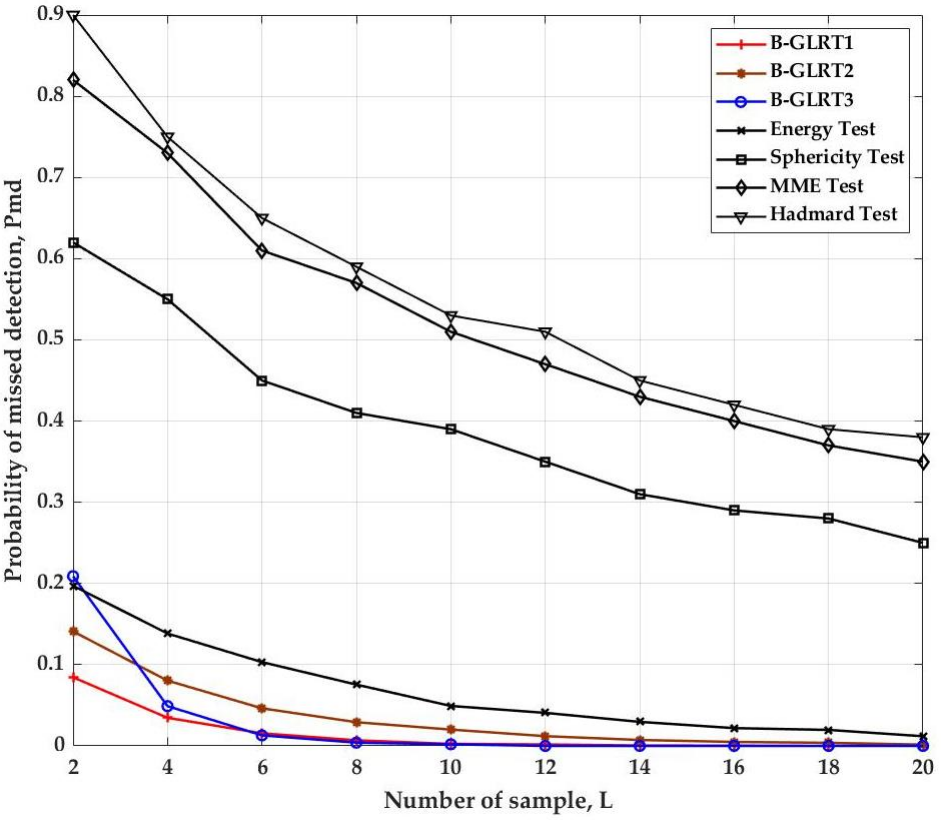

Figure 5. Probability of missed detection of the proposed approach versus L where a pfa = 5×10^{-1}, an average SNR = –3 dB.

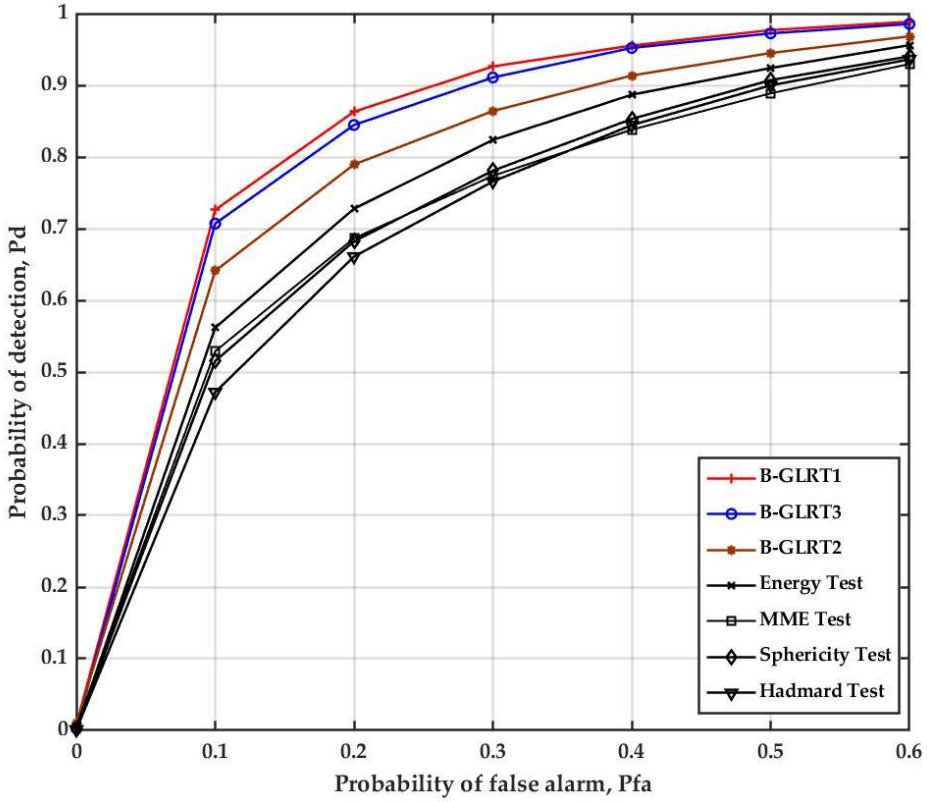

Figure 6. Probability of detection versus probability of false alarm at SNR = −3 dB, $N_r = 3$, $N_t = 2$ and $L = 20$.

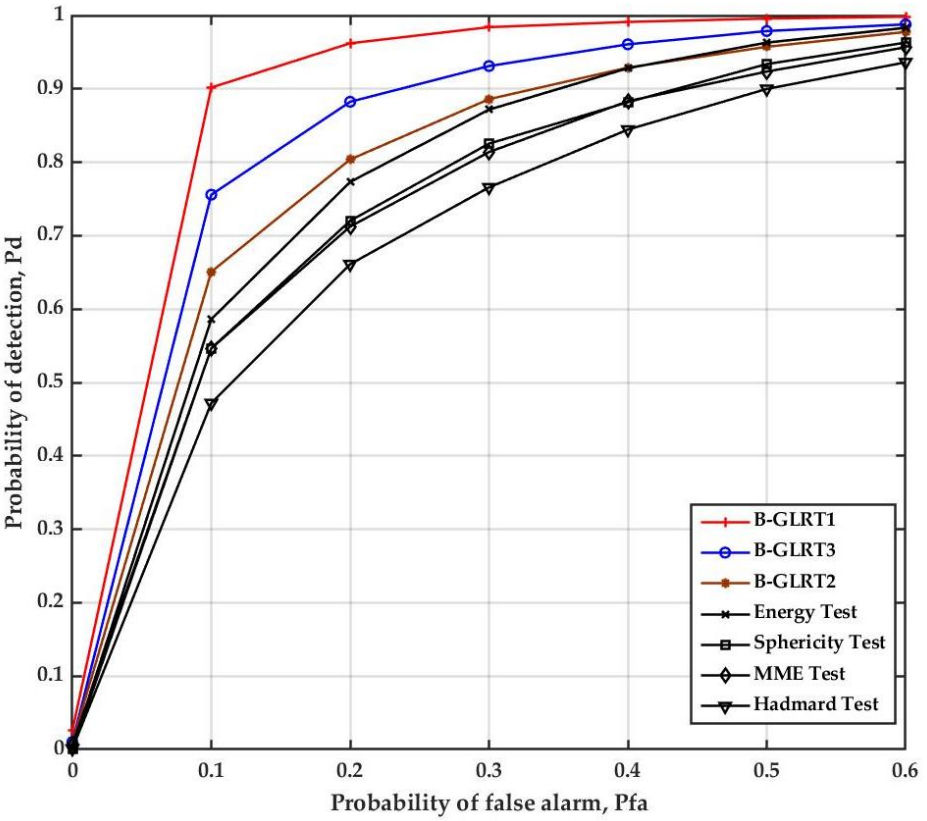

Figure 7. Probability of detection against probability of false alarm at SNR = – 3 dB, $N_r = 5$, $N_t = 3$ and $L = 25$.

Finally, we show the probability of missed detection of the detectors in terms of SNR where the number of samples is changed, as shown in Figure 8. From this figure, it can be seen that the proposed detectors have a significant performance improvement in terms of the probability of missed detection when the number of signal samples is increased.

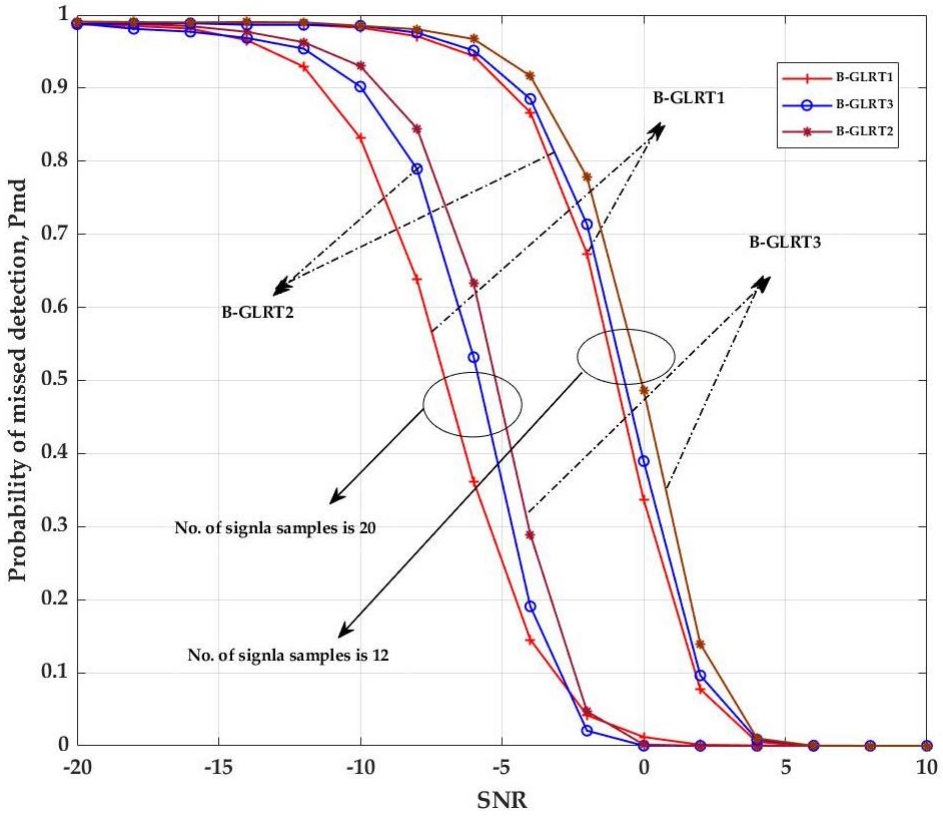

Figure 8. Probability of missed detection for the detectors versus a SNR with $Pfa = 5 \times 10^{-1}$, $N_r = 3$, $N_t = 2$.

6. Conclusions

This paper presents a novel method for developing spectrum sensing detectors in multicell CR network with non-perfect CSI for the SU network. In this context, novel detection schemes such as the B-GLRT1, B-GLRT2, and B-GLRT3 are proposed for different cases when the noise distribution parameters are unknown in the non-perfect channel. For the first case with unknown noise covariance and the perfect channel, we derived a GLRT1-based binary hypothesis detector for spectrum sensing in MIMO CR networks. In this case, our formulation for maximizing likelihood distribution determines the corresponding unknown parameters for each hypothesis within a specified amount of SNR from the SU base stations. We further developed an expression of B-GLRT2 and B-GLRT3, where the CSI uncertainty in MIMO cognitive radio is not perfect. This problem is formulated as an optimization problem that is solved in different ways to obtain a robust and sub-optimal solution for the spectrum sensing CR. Simulation results are presented to demonstrate the proposed detectors' performance where a CSI and noise uncertainty is available with a finite number of observed data samples. The results also illustrate that the proposed B-GLRT detectors achieve significant improvement compared with state-of-the-art spectrum sensing schemes. We present simulation results showing that our solution methods outperform state-of-the-art methods with existing and non-existing channel uncertainty. Furthermore, the theoretical analysis and simulation results indicate that our approaches can offer outstanding spectrum sensing performance when small sample size is available.This work focused on obtaining a robust signal detector at the secondary user based on local decisions received from the cooperating signal PU considering CSI

uncertainty in MIMO CR Networks. A promising extension to future work can use the cooperative spectrum sensing at the fusion center side in the presence of the noise and channel uncertainty.

Author Contributions: Conceptualization, M.A.-A. and N.E.I.; methodology, M.A.-A., A.A.-A.; software, M.A.F.; validation, M.A.F., A.A.-A., A.A.-D., L.A., R.G.M., A.J.H. and L.F.; data Creation, M.A.F.; writing—original draft preparation, M.A.F. and N.E.I.; writing—review and editing: A.A.-A., A.J.H., L.A., A.A.-D., M.A.F., L.F. and R.G.M.; revised version M.A.F., A.J.H.; supervision, N.E.I. All authors have read and agreed to the published version of the manuscript.

Funding: This research received no external funding.

Conflicts of Interest: The authors declare that they have no conflict of interest.

Appendix A

Appendix A.1

1. Equation (24) can be written equivalently as

$$\begin{aligned}\mathbf{R}_{\eta} &= \underset{\substack{\boldsymbol{\Gamma}_0:Diagonal \\ \mathbf{M}:Diagonal \\ \boldsymbol{\Psi}\geq 0}}{\operatorname{argmax}} \; (L|\boldsymbol{\Psi}| - tr\{\mathbf{R}\boldsymbol{\Psi}\} \\ &\quad +(\alpha+1)\log|\mathbf{M}| - etr[\mathbf{B}\mathbf{M}])\end{aligned}$$

subject to

$$\begin{aligned}\boldsymbol{\Gamma}_1^{-1} &\leq \boldsymbol{\Psi} \\ \boldsymbol{\Gamma}_0^{-1} &\leq \mathbf{M} \\ \mathbf{M} &\geq \boldsymbol{\Psi}.\end{aligned}$$

This problem can be solved by using Schur complement as shown in our previous work in [32]:

$$\begin{bmatrix} \boldsymbol{\Psi} & \mathbf{I} \\ \mathbf{I} & \mathbf{R}_{\eta} + \underbrace{(\widehat{\mathbf{R}}_h + \boldsymbol{\Delta}\mathbf{R}_h)}_{\mathbf{R}_h} \end{bmatrix} \geq 0$$

Similarly,

$$\begin{bmatrix} \mathbf{M} & \mathbf{I} \\ \mathbf{I} & \mathbf{R}_{\eta} \end{bmatrix} \geq 0$$

2. In sub-optimal method (B-GLRT2), $\boldsymbol{\Delta}\mathbf{R}_h$ is equal to $+\epsilon\mathbf{I}_{Nr}$ then problem reduces to

$$\begin{aligned}\mathbf{R}_{\eta} &= \underset{\substack{\boldsymbol{\Gamma}_0:Diagonal \\ \mathbf{M}:Diagonal \\ \boldsymbol{\Psi}\geq 0}}{\operatorname{argmax}} \; (L|\boldsymbol{\Psi}| - tr\{\mathbf{R}\boldsymbol{\Psi}\} \\ &\quad +(\alpha+1)\log|\mathbf{M}| - etr[\mathbf{B}\mathbf{M}])\end{aligned}$$

subject to

$$\begin{bmatrix} \boldsymbol{\Psi} & \mathbf{I} \\ \mathbf{I} & \mathbf{R}_{\eta} + \underbrace{(\widehat{\mathbf{R}}_h + \epsilon\mathbf{I}_{Nr})}_{\mathbf{R}_h} \end{bmatrix} \geq 0$$

$$\begin{bmatrix} \mathbf{M} & \mathbf{I} \\ \mathbf{I} & \mathbf{R}_{\eta} \end{bmatrix} \geq 0$$

$$\mathbf{M} \geq \boldsymbol{\Psi}$$

Appendix A.2

1. Solving for $\mathbf{\Gamma}_0$, the problem in Equation (30) reduced to *P*8:

$$\begin{aligned} P8 \quad : \quad & \underset{\Gamma_0:Diagonal}{\operatorname{argmax}} \ (L\log|\mathbf{R}_h+\mathbf{\Gamma}_0|^{-1} \\ & -tr[\mathbf{R}(\mathbf{R}_h+\mathbf{\Gamma}_0)_1^{-1}] \\ & +(\rho+1)\log\left|\mathbf{\Gamma}_0^{-1}\right| - tr[\mathbf{B}\mathbf{\Gamma}_0^{-1}]) \end{aligned}$$

subject to

$$\begin{gathered} (\mathbf{R}_h+\mathbf{\Gamma}_0)^{-1} \leq \mathbf{\Psi} \\ \mathbf{\Gamma}_0^{-1} \leq \mathbf{M} \\ \mathbf{M} \geq \mathbf{\Psi}. \end{gathered}$$

This problem can be solved according to the solution that is mentioned in Appendix A.1.

2. Back to Equation (30) to solve for $\Delta\mathbf{R}_h$, the problem reduce to:

$$\begin{aligned} P9 \quad : \quad & \underset{\Delta\mathbf{R}_h}{\operatorname{argmax}}(L\log|(\Re+\mathbf{\Delta R}_h)|^{-1} \\ & -tr[\mathbf{R}(\Re+\mathbf{\Delta R}_h)^{-1}] \\ & +(\rho+1)\log\left|\mathbf{\Gamma}_0^{-1}\right| - tr[\mathbf{K}\mathbf{\Gamma}_0^{-1}]) \end{aligned}$$

subject to

$$(\Re+\mathbf{\Delta R}_h)^{-1} \leq \mathbf{\Psi} \ \|\mathbf{\Delta R}_h\|_F \leq \epsilon.$$

This equation can also be solved using Schur complement; the problem will becomes:

$$\begin{bmatrix} \mathbf{\Psi} & \mathbf{I} \\ \mathbf{I} & (\Re+\mathbf{\Delta R}_h) \end{bmatrix} \geq 0$$

References

1. Guo, C.; He, W.; Li, G.Y. Optimal Fairness-Aware Resource Supply and Demand Management for Mobile Edge Computing. *IEEE Wirel. Commun. Lett.* **2020**. [CrossRef]
2. Mehrabian, A.; Zaimbashi, A. Robust and blind eigenvalue-based multiantenna spectrum sensing under IQ imbalance. *IEEE Trans. Wirel. Commun.* **2018**, *17*, 5581–5591. [CrossRef]
3. Miridakis, N.I.; Tsiftsis, T.A.; Alexandropoulos, G.C. MIMO underlay cognitive radio: Optimized power allocation, effective number of transmit antennas and harvest-transmit tradeoff. *IEEE Trans. Green Commun. Netw.* **2018**, *2*, 1101–1114. [CrossRef]
4. Wang, N.; Han, S.; Lu, Y.; Zhu, J.; Xu, W. Distributed Energy Efficiency Optimization for Multi-User Cognitive Radio Networks Over MIMO Interference Channels: A Non-Cooperative Game Approach. *IEEE Access* **2020**, *8*, 26701–26714. [CrossRef]
5. Shi, Z.; Xie, X.; Lu, H. Deep reinforcement learning based intelligent user selection in massive mimo underlay cognitive radios. *IEEE Access* **2019**, *7*, 110884–110894. [CrossRef]
6. Zhao, X.; Riaz, S.; Geng, S. A reconfigurable MIMO/UWB MIMO antenna for cognitive radio applications. *IEEE Access* **2019**, *7*, 46739–46747. [CrossRef]
7. Rao, P.R.M.; Sangeetha, M. Calculation of Capacity, Spectral Efficiency, Bit Error Rate in Chaotic Cognitive Radio System with Subcarrier Shifting in OFDM-MIMO. In Proceedings of the 2018 International Conference on Communication and Signal Processing (ICCSP), Chennai, India, 3–5 April 2018; pp. 0504–0507.
8. Haykin, S. Cognitive radar networks. In Proceedings of the 1st IEEE International Workshop on Computational Advances in Multi-Sensor Adaptive Processing, Puerto Vallarta, Mexico, 13–15 December 2005; pp. 1–20.
9. Chen, A.Z.; Shi, Z.P.; Sun, H.; He, Z.Q.; Bu, F.; Yang, D. A low-complexity spectrum sensing method for noncircular signal in cognitive radio networks with multiple receive antennas. *IEEE Commun. Lett.* **2019**, *23*, 1190–1193. [CrossRef]
10. Badawy, A.; El Shafie, A.; Khattab, T. On the performance of quickest detection spectrum sensing: The case of cumulative sum. *IEEE Commun. Lett.* **2020**, *24*, 739–743. [CrossRef]
11. Hu, L.; Shi, R.; Mao, M.; Chen, Z.; Zhou, H.; Li, W. Optimal energy-efficient transmission for hybrid spectrum sharing in cooperative cognitive radio networks. *China Commun.* **2019**, *16*, 150–161. [CrossRef]

12. Yin, W.; Chen, H. Decision-Driven Time-Adaptive Spectrum Sensing in Cognitive Radio Networks. *IEEE Trans. Wirel. Commun.* **2020**, *19*, 2756–2769. [CrossRef]
13. Zhang, J.; Liu, L.; Liu, M.; Yi, Y.; Yang, Q.; Gong, F. Mimo spectrum sensing for cognitive radio-based internet of things. *IEEE Internet Things J.* **2020**, *7*, 8874–8885. [CrossRef]
14. Li, X.; Zhu, Q.; Wang, X. Privacy-Aware Crowdsourced Spectrum Sensing and Multi-User Sharing Mechanism in Dynamic Spectrum Access Networks. *IEEE Access* **2019**, *7*, 32971–32988. [CrossRef]
15. Cai, P.; Zhang, Y. Intelligent cognitive spectrum collaboration: Convergence of spectrum sensing, spectrum access, and coding technology. *Intell. Converg. Netw.* **2020**, *1*, 79–98. [CrossRef]
16. Xiong, T.; Yao, Y.D.; Ren, Y.; Li, Z. Multiband spectrum sensing in cognitive radio networks with secondary user hardware limitation: Random and adaptive spectrum sensing strategies. *IEEE Trans. Wirel. Commun.* **2018**, *17*, 3018–3029. [CrossRef]
17. Alhamad, R.I. Optimal Power Allocation for Cooperative Spectrum Sensing. In Proceedings of the 2019 IEEE International Symposium on Dynamic Spectrum Access Networks (DySPAN), Newark, NJ, USA, 11–14 November 2019; pp. 1–5.
18. Xing, H.; Zheng, D.; Wang, S. Mobility Improves the Performance of Collaborated Spectrum Sensing. In Proceedings of the 2020 IEEE/CIC International Conference on Communications in China (ICCC), Chongqing, China, 9–11 August 2020; pp. 864–868.
19. Zhang, X.; Ma, Y.; Gao, Y.; Zhang, W. Autonomous compressive-sensing-augmented spectrum sensing. *IEEE Trans. Veh. Technol.* **2018**, *67*, 6970–6980. [CrossRef]
20. Axell, E.; Leus, G.; Larsson, E.G.; Poor, H.V. Spectrum sensing for cognitive radio: State-of-the-art and recent advances. *IEEE Signal Process. Mag.* **2012**, *29*, 101–116. [CrossRef]
21. Stöckle, C.; Munir, J.; Mezghani, A.; Nossek, J.A. Channel estimation in massive MIMO systems using 1-bit quantization. In Proceedings of the 2016 IEEE 17th International Workshop on Signal Processing Advances in Wireless Communications (SPAWC), Edinburgh, UK, 3–6 July 2016; pp. 1–6.
22. Kaur, R.; Kumar, D. Multiple-Input Multiple-Output (MIMO) Cognitive Radio User Selection Using Channel State Information at Transmitter (CSIT). In Proceedings of the 2018 International Conference on Inventive Research in Computing Applications (ICIRCA), Coimbatore, India, 11–12 July 2018; pp. 25–30.
23. Chaudhary, R.K.; Thummaluru, S.R. Reconfigurable MIMO Filtenna for Spectrum Underlay Cognitive Radio. In Proceedings of the 2019 PhotonIcs & Electromagnetics Research Symposium-Spring (PIERS-Spring), Rome, Italy, 17–20 June 2019; pp. 582–586.
24. Shehata, H.; Khattab, T. Energy detection spectrum sensing in full-duplex cognitive radio: The practical case of rician RSI. *IEEE Trans. Commun.* **2019**, *67*, 6544–6555. [CrossRef]
25. López-Valcarce, R.; Vazquez-Vilar, G.; Sala, J. Multiantenna spectrum sensing for cognitive radio: Overcoming noise uncertainty. In Proceedings of the 2010 2nd International Workshop on Cognitive Information Processing, Elba, Italy, 14–16 June 2010; pp. 310–315.
26. Yang, X.; Peng, S.; Zhu, P.; Hongyang, C.; Cao, X. Effect of correlations on the performance of GLRT detector in cognitive radios. *IEICE Trans. Commun.* **2011**, *94*, 1089–1093. [CrossRef]
27. Ciuonzo, D.; De Maio, A.; Orlando, D. A unifying framework for adaptive radar detection in homogeneous plus structured interference—Part I: On the maximal invariant statistic. *IEEE Trans. Signal Process.* **2016**, *64*, 2894–2906. [CrossRef]
28. Sedighi, S.; Taherpour, A.; Sala Álvarez, J.; Khattab, T. On the performance of Hadamard ratio detector-based spectrum sensing for cognitive radios. *IEEE Trans. Signal Process.* **2015**, *63*, 3809–3824. [CrossRef]
29. Stoica, P.; Babu, P. On the exponentially embedded family (EEF) rule for model order selection. *IEEE Signal Process. Lett.* **2012**, *19*, 551–554. [CrossRef]
30. Kallummil, S.; Kalyani, S. High SNR consistent linear model order selection and subset selection. *IEEE Trans. Signal Process.* **2016**, *64*, 4307–4322. [CrossRef]
31. Ge, D.; Zeng, X.J. Functional Fuzzy System: A Nonlinear Regression Model and Its Learning Algorithm for Function-on-Function Regression. *IEEE Trans. Fuzzy Syst.* **2021**. [CrossRef]
32. Sedighi, S.; Taherpour, A.; Monfared, S.S. Bayesian generalised likelihood ratio test-based multiple antenna spectrum sensing for cognitive radios. *IET Commun.* **2013**, *7*, 2151–2165. [CrossRef]
33. Al-Amidie, M.; Al-Asadi, A.; Micheas, A.C.; Islam, N.E. Spectrum sensing based on Bayesian generalised likelihood ratio for cognitive radio systems with multiple antennas. *IET Commun.* **2018**, *13*, 305–311. [CrossRef]
34. Kim, J.; Choi, J.P. Sensing coverage-based cooperative spectrum detection in cognitive radio networks. *IEEE Sens. J.* **2019**, *19*, 5325–5332. [CrossRef]
35. Foschini, G.J.; Gans, M.J. On limits of wireless communications in a fading environment when using multiple antennas. *Wirel. Pers. Commun.* **1998**, *6*, 311–335. [CrossRef]
36. Vishwanath, S.; Jindal, N.; Goldsmith, A. Duality, achievable rates, and sum-rate capacity of Gaussian MIMO broadcast channels. *IEEE Trans. Inf. Theory* **2003**, *49*, 2658–2668. [CrossRef]
37. Gazestani, A.H.; Ghorashi, S.A. Distributed diffusion-based spectrum sensing for cognitive radio sensor networks considering link failure. *IEEE Sen. J.* **2018**, *18*, 8617–8625.
38. Jin, Z.; Yao, K.; Lee, B.; Cho, J.; Zhang, L. Channel status learning for cooperative spectrum sensing in energy-restricted cognitive radio networks. *IEEE Access* **2019**, *7*, 64946–64954. [CrossRef]
39. Vaze, C.S.; Varanasi, M.K. On the achievable rate of the fading dirty paper channel with imperfect CSIT. In Proceedings of the 2009 43rd Annual Conference on Information Sciences and Systems, Baltimore, MD, USA, 18–20 March 2009; pp. 346–351.

40. Vaze, C.S.; Varanasi, M.K. Dirty paper coding for fading channels with partial transmitter side information. In Proceedings of the 2008 42nd Asilomar Conference on Signals, Systems and Computers, Pacific Grove, CA, USA, 26–29 October 2008; pp. 341–345.
41. Vaze, C.S.; Varanasi, M.K. Dirty paper coding for the MIMO cognitive radio channel with imperfect CSIT. In Proceedings of the 2009 IEEE International Symposium on Information Theory, Seoul, Korea, 28 June–3 July 2009; pp. 2532–2536.
42. Tran, L.N.; Juntti, M.; Bengtsson, M.; Ottersten, B. Weighted sum rate maximization for MIMO broadcast channels using dirty paper coding and zero-forcing methods. *IEEE Trans. Commun.* **2013**, *61*, 2362–2373. [CrossRef]
43. Na, W.; Yoon, J.; Cho, S.; Griffith, D.; Golmie, N. Centralized cooperative directional spectrum sensing for cognitive radio networks. *IEEE Trans. Mob. Comput.* **2017**, *17*, 1260–1274. [CrossRef]
44. Patel, A.; Tripathi, B.; Jagannatham, A.K. Robust Estimator-Correlator for Spectrum Sensing in MIMO CR Networks with CSI Uncertainty. *IEEE Wirel. Commun. Lett.* **2014**, *3*, 253–256. [CrossRef]
45. Kay, S.M. *Fundamentals of Statistical Signal Processing: Practical Algorithm Development*; Pearson Education: London, UK, 2013; Volume 3.
46. Enderlein, G.; Wilks, S.S. Mathematical Statistics. *Biom. Z.* **1964**, *6*, 214–215. [CrossRef]
47. Moustakides, G.V. Finite sample size optimality of GLR tests. *arXiv* **2009**, arXiv:0903.3795.
48. Taherpour, A.; Nasiri-Kenari, M.; Gazor, S. Multiple antenna spectrum sensing in cognitive radios. *IEEE Trans. Wirel. Commun.* **2010**, *9*, 814–823. [CrossRef]
49. Gelman, A.; Carlin, J.B.; Stern, H.S.; Dunson, D.B.; Vehtari, A.; Rubin, D.B. *Bayesian Data Analysis*; Chapman and Hall/CRC: Boca Raton, FL, USA, 2013.
50. Grant, M.; Boyd, S.; Ye, Y. CVX: Matlab Software for Disciplined Convex Programming, 2008. Available online: http://stanford.edu/boyd/cvx (accessed on 12 August 2020).
51. Schad, A.; Pesavento, M. Max-min fair transmit beamforming for multi-group multicasting. In Proceedings of the 2012 International ITG Workshop on Smart Antennas (WSA), Dresden, Germany, 7–8 March 2012; pp. 115–118.
52. Liu, L.; Fan, L. The complexity analysis of an efficient interior-point algorithm for linear optimization. In Proceedings of the 2010 Third International Joint Conference on Computational Science and Optimization, Huangshan, China, 28–31 May 2010; Volume 2, pp. 21–24.
53. Al-Asadi, A.; Al-Amidie, M.; Micheas, A.C.; McGarvey, R.G.; Islam, N.E. Worst case fair beamforming for multiple multicast groups in multicell networks. *IET Commun.* **2018**, *13*, 664–671. [CrossRef]
54. Al-Ali, M.; Ho, K. Transmit Precoding in Underlay MIMO Cognitive Radio with Unavailable or Imperfect Knowledge of Primary Interference Channel. *IEEE Trans. Wirel. Commun.* **2016**. [CrossRef]
55. Sharma, S.K.; Chatzinotas, S.; Ottersten, B. SNR estimation for multi-dimensional cognitive receiver under correlated channel/noise. *IEEE Trans. Wirel. Commun.* **2013**, *12*, 6392–6405. [CrossRef]
56. Zhou, F.; Beaulieu, N.C. An improved and more accurate expression for a PDF related to eigenvalue-based spectrum sensing. *IEEE Syst. J.* **2018**, *13*, 1320–1323. [CrossRef]
57. Ramírez, D.; Vazquez-Vilar, G.; López-Valcarce, R.; Vía, J.; Santamaría, I. Detection of rank-*P* signals in cognitive radio networks with uncalibrated multiple antennas. *IEEE Trans. Signal Process.* **2011**, *59*, 3764–3774. [CrossRef]